Received: 16 March 2022 | Revised: 21 June 2022 | Accepted: 4 July 2022

DOI: 10.1111/mpp.13249

Molecular Plant Pathology WILEY

ORIGINAL ARTICLE

Transcriptome analyses unveiled differential regulation of AGO and DCL genes by pepino mosaic virus strains

Cristina Alcaide | Livia Donaire | Miguel A. Aranda

Department of Stress Biology and Plant Pathology, Centro de Edafología y Biología Aplicada del Segura-CSIC, Murcia, Spain

Correspondence
Miguel A. Aranda, Department of Stress Biology and Plant Pathology, Centro de Edafología y Biología Aplicada del Segura-CSIC, Murcia, Spain.
Email: m.aranda@cebas.csic.es

Funding information
Spanish Ministry of Science and Innovation, Grant/Award Number: FPU16/02569 and RTI2018-097099-B-100

Abstract

Pepino mosaic virus (PepMV) is a single-stranded (ss), positive-sense (+) RNA potexvirus that affects tomato crops worldwide. We have described an in planta antagonistic interaction between PepMV isolates of two strains in which the EU isolate represses the accumulation of the CH2 isolate during mixed infections. Reports describing transcriptomic responses to mixed infections are scant. We carried out transcriptomic analyses of tomato plants singly and mixed-infected with two PepMV isolates of both strains. Comparison of the transcriptomes of singly infected plants showed that deeper transcriptomic alterations occurred at early infection times, and also that each of the viral strains modulated the host transcriptome differentially. Mixed infections caused transcriptomic alterations similar to those for the sum of single infections at early infection times, but clearly differing at later times postinfection. We next tested the hypothesis that PepMV-EU, in either single or mixed infections, deregulates host gene expression differentially so that virus accumulation of both strains gets repressed. That seemed to be the case for the genes *AGO1a*, *DCL2d*, *AGO2a*, and *DCL2b*, which are involved in the antiviral silencing pathway and were upregulated by PepMV-EU but not by PepMV-CH2 at early times postinfection. The pattern of *AGO2a* expression was validated by reverse transcription-quantitative PCR in tomato and *Nicotiana benthamiana* plants. Using an *N. benthamiana ago2* mutant line, we showed that *AGO2* indeed plays an important role in the antiviral defence against PepMV, but it is not the primary determinant of the outcome of the antagonistic interaction between the two PepMV strains.

KEYWORDS
mixed infections, potexvirus, RNAi, tomato

1 | INTRODUCTION

Mixed viral infections are very common in nature and can lead to virus–virus interactions with diverse outcomes (Sanjuán, 2021). Likewise, during infection, virus–host interactions necessarily occur, and these can be influenced by the type of infection (single or mixed) and the interactions that mixed-infecting viruses may establish between themselves. Virus infections cause deep alterations of the host transcriptome (Gómez-Aix et al., 2016; Hanssen et al., 2011; Li et al., 2018; Lu et al., 2012; Seo et al., 2018), and thus the type of infection and potential virus–virus interactions may have a differential impact on the transcriptomes. Mixed infections with viruses from

different species have been studied for a large variety of systems (Jones, 2021; Moreno & López-Moya, 2020), although much less is known about interactions among viruses of the same species belonging to different strains.

For plants, in epidemiological and evolutionary terms, one of the best-studied examples of mixed strain infections is pepino mosaic virus (PepMV) (Gómez et al., 2009, 2012; Gómez-Aix et al., 2019; Hanssen & Thomma, 2010; Ling et al., 2013; Pagán et al., 2006). PepMV is a single-stranded (ss), positive-sense (+) RNA potexvirus that affects tomato crops worldwide (Hanssen & Thomma, 2010). The PepMV diversity comprises five strains: the European (EU), the Chilean (CH2), the North American (US1/CH1), the original Peruvian (LP), and the new Peruvian (PES) (Hanssen & Thomma, 2010; Moreno-Perez et al., 2014). PepMV was first described affecting tomato crops in the Netherlands (van der Vlugt et al., 2000). At the beginning of the epidemics, PepMV populations were composed of EU isolates, but from the year 2005 onwards, PepMV populations mainly shifted to isolates of the CH2 strain, although isolates of the EU strain persisted in mixed infections (Alcaide et al., 2020; Gómez et al., 2009; Gómez-Aix et al., 2019; Hanssen et al., 2008; Ling et al., 2013; Pagán et al., 2006). Thus, the CH2 strain became predominant but did not completely displace the EU strain. It was also shown that isolates belonging to the CH2 strain have reduced in planta fitness in simultaneous mixed infections with isolates of the EU strain, while simultaneous mixed infections had no effect on the fitness of the EU isolates, defining an asymmetric antagonistic relationship between the viruses involved (Alcaide et al., 2020; Alcaide & Aranda, 2021; Gómez et al., 2009).

The PepMV genome is approximately 6.4 kb in length, with five open reading frames (ORFs), two untranslated regions at the 5′ and the 3′ ends, and a poly (A) tail at the 3′ end (Aguilar et al., 2002). ORF1 encodes an RNA-dependent RNA polymerase (RdRp) containing three conserved domains (methyltransferase, helicase, and polymerase domains). ORFs 2, 3, and 4 encode the triple gene block proteins, TGB1, TGB2, and TGB3, involved in the intra- and intercellular movement of the virus (Morozov & Solovyev, 2003; Solovyev et al., 2012; Tilsner et al., 2013). TGB1 has also been described as a potexvirus silencing suppressor (Bayne et al., 2005; Park et al., 2014). ORF5 encodes the capsid protein (CP), the subunit that oligomerizes to form the viral capsid (Agirrezabala et al., 2015), which is involved in the cell-to-cell and long-distance movement of the virus (Morozov & Solovyev, 2003; Sempere et al., 2011) and has also been described as a silencing suppressor (Mathioudakis et al., 2014). In addition, TGBs and CP take part in the formation of the viral replication complexes (Linnik et al., 2013; Tilsner et al., 2013).

Transcriptomic alterations of tomato plants associated with PepMV infections have been described using a tomato GeneChip microarray (Hanssen et al., 2011). Different responses were observed after single infection with each of two PepMV isolates of the CH2 strain that differ in symptom aggressiveness but not in virus accumulation in the host. In general terms, PepMV infection resulted in repression of photosynthesis genes and stronger activation of defences by the aggressive isolate. Interestingly, PepMV seemed to deregulate the RNA silencing pathway (Hanssen et al., 2011). It is well known that RNA silencing is central for plant defence (Baulcombe, 2004). During viral infections, double-stranded RNAs (dsRNAs) are produced from different viral origins and are processed by RNase III Dicer-like (DCL) proteins into 21 to 24 nucleotide virus-derived small interfering RNAs (vsiRNAs) (Ding, 2010). Then, vsiRNAs can be incorporated into effector complexes called RNA-induced silencing complexes (RISC), where one strand of a vsiRNA can be loaded onto an Argonaute (AGO) protein (Ding & Voinnet, 2007; Pantaleo et al., 2007), being used as a guide by the AGO protein, which cleaves target ssRNAs (Tolia & Joshua-Tor, 2007). There are also host RNA-dependent RNA polymerases (RDRs) that participate in the silencing pathway, which are able to amplify the silencing signal, thereby providing short- and long-distance RNA silencing effects (Pumplin & Voinnet, 2013; Voinnet, 2005). Plant genomes encode several members of each of these protein families, with a subset of them having demonstrated antiviral functions. For instance, in *Arabidopsis thaliana*, antiviral functions have been attributed to AGO1, AGO2, AGO4, AGO5, AGO7, and AGO10 (Carbonell & Carrington, 2015), with AGO1 and AGO2 as the main antiviral AGOs against RNA viruses. Roles in antiviral defence have also been attributed to DCL2 and DCL4 (Katsarou et al., 2019; Liu et al., 2009; Xie et al., 2004), and to RDRs, mainly RDR1 and RDR6 (Donaire et al., 2008; Wassenegger & Krczal, 2006; Willmann et al., 2011).

Although interactions between PepMV strains have been well documented, the effects that they may have on the host transcriptome have not been studied thus far. In fact, despite mixed infections being widespread in nature, there are only a few reports comparing the host response to single versus mixed viral infections (Bednarek et al., 2021; Ding et al., 2019; Seo et al., 2018), with no studies describing transcriptome alterations caused by two strains of the same virus reported before. The PepMV/tomato experimental system, where we have described an asymmetric antagonism between PepMV strains, allows for a hypothesis-driven study providing novel insights on viral antagonism. The present work seeks to describe the transcriptomic responses of tomato plants to PepMV single and mixed infections, with a particular focus on genes encoding the RNA silencing pathway components. It also seeks to demonstrate that the outcome of the virus–virus interaction described for PepMV in tomato also takes place in the model host *Nicotiana benthamiana*, paving the way to its further and efficient mechanistic dissection.

2 | RESULTS

2.1 | Virus accumulation in single and mixed-infected MicroTom plants at different times postinoculation

MicroTom plants were mock, single, or mixed inoculated with PepMV-EU and PepMV-CH2. Plants were sampled, RNA was extracted and virus accumulation was quantified at 7, 14, and 21 days

postinoculation (dpi) (Figure 1). In the case of PepMV-EU, no significant differences were found between single and mixed infections at any of the sampling times (Figure 1a). When comparing PepMV-EU accumulation at different times postinoculation, significant differences were found among the different time points, with a higher accumulation at 7 dpi with respect to 14 dpi ($F = 50.13$, $p < 0.001$) or to 21 dpi ($F = 71.87$, $p < 0.001$), and also a higher accumulation at 14 dpi with respect to 21 dpi ($F = 9.79$, $p = 0.011$). Regarding the accumulation of PepMV-CH2, significant differences were found between single and mixed infections at 7 dpi ($F = 10.95$, $p = 0.030$) and 14 dpi ($F = 15.90$, $p = 0.016$), but not at 21 dpi ($F = 3.521$, $p = 0.134$) (Figure 1b). No differences in virus accumulation were found between the different sampling times for PepMV-CH2 in single infections, but an accumulation increase with time was found for mixed infections. These results agree with our previous observations using other tomato cultivars (Alcaide & Aranda, 2021; Gómez et al., 2009), and reinforce the idea of an asymmetric antagonism between both viruses at least in tomato, which in MicroTom plants appeared to be particularly evident at early times after mixed infection.

2.2 | Transcriptome sequencing

Ribosomal RNA-depleted RNA Illumina TruSeq libraries were sequenced for each of the treatments described above: mock, PepMV-EU, PepMV-CH2, and PepMV-EU + -CH2-inoculated plants sampled at 7, 14, and 21 dpi. The number of reads was between 41,223,918 and 57,626,242, and the percentage of reads after trimming and quality filtering was more than 99.9% in all the samples. The percentage of mapped reads against the tomato genome varied between 84.2% and 99.8%, being higher in the mock samples as compared with infected samples (Table S1), probably due to the presence of reads of the viral genome. The percentage of mapped reads against the tomato transcriptome ranged between 59.8% and 93.3% (Table S1). A principal component analysis was performed to test whether samples were grouped by type or time of infection (Figure 2a). A clear differentiation among the different sampling times was observed. Also, a clear differentiation was found regarding the type of infection, with less variation between PepMV-CH2 single and mixed infection, especially at 7 dpi (Figure 2a). We studied the differentially expressed genes (DEGs) between mock and infected plants, and found a larger number of up-regulated versus down-regulated genes (Figure 2b). For single infections, the largest number of up-regulated genes was at 7 dpi for PepMV-CH2, whereas for mixed infections more up-regulated genes were found at 14 and 21 dpi (Figure 2b). Only two down-regulated genes were found in single PepMV-EU-infected plants. In the case of PepMV-CH2 and mixed infections, the largest number of down-regulated genes was found at 14 dpi (Figure 2b). At 7 dpi we found the same number (33) of shared up-regulated genes for PepMV-EU and mixed infections

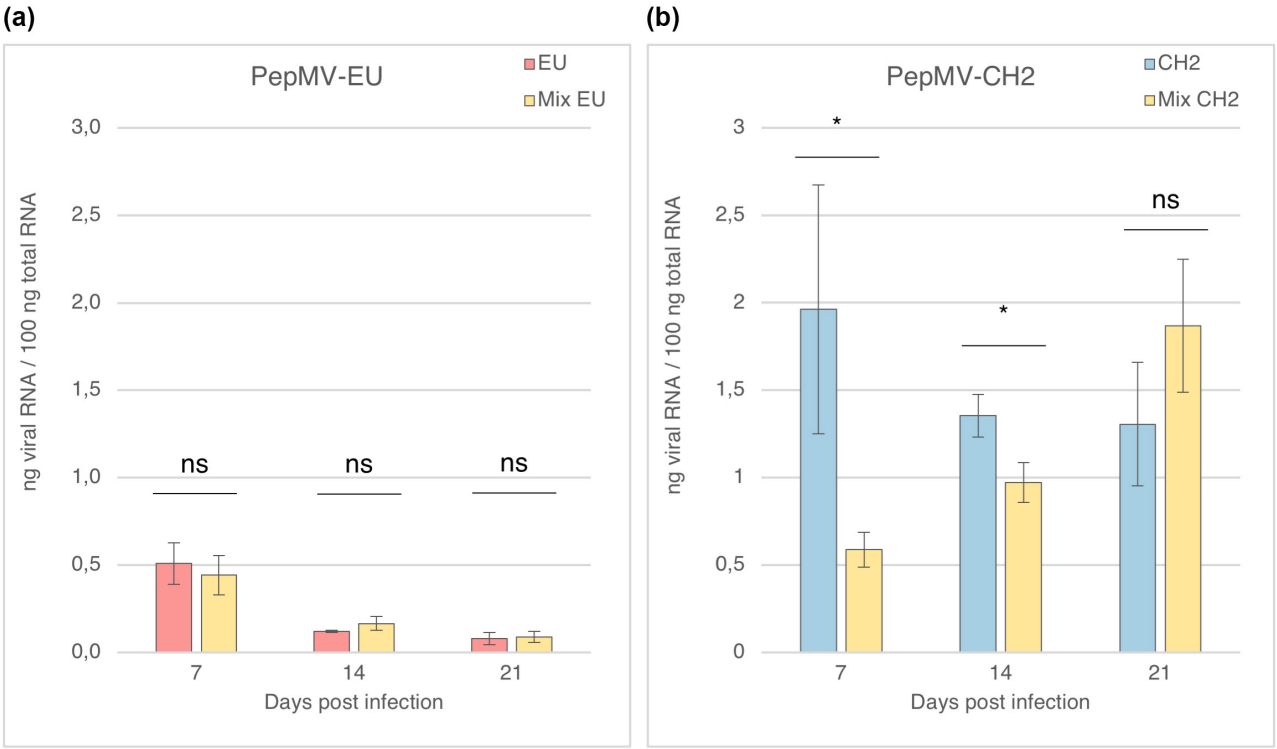

FIGURE 1 PepMV accumulation in MicroTom plants. (a) Accumulation of PepMV-EU in single (red) and mixed (orange) infections at different times postinoculation (7, 14, and 21 days postinoculation [dpi]). (b) Accumulation of PepMV-CH2 in single (blue) and mixed (orange) infections at different times postinoculation (7, 14, and 21 dpi). Virus accumulation was determined in pools of three plants for each time point by absolute reverse transcription-quantitative PCR and shown as nanograms of viral RNA/100 ng total RNA; each bar represents the mean and its standard deviation. Each treatment had three biological replicates. Asterisks show significance level (*$p < 0.05$; ns = not significant).

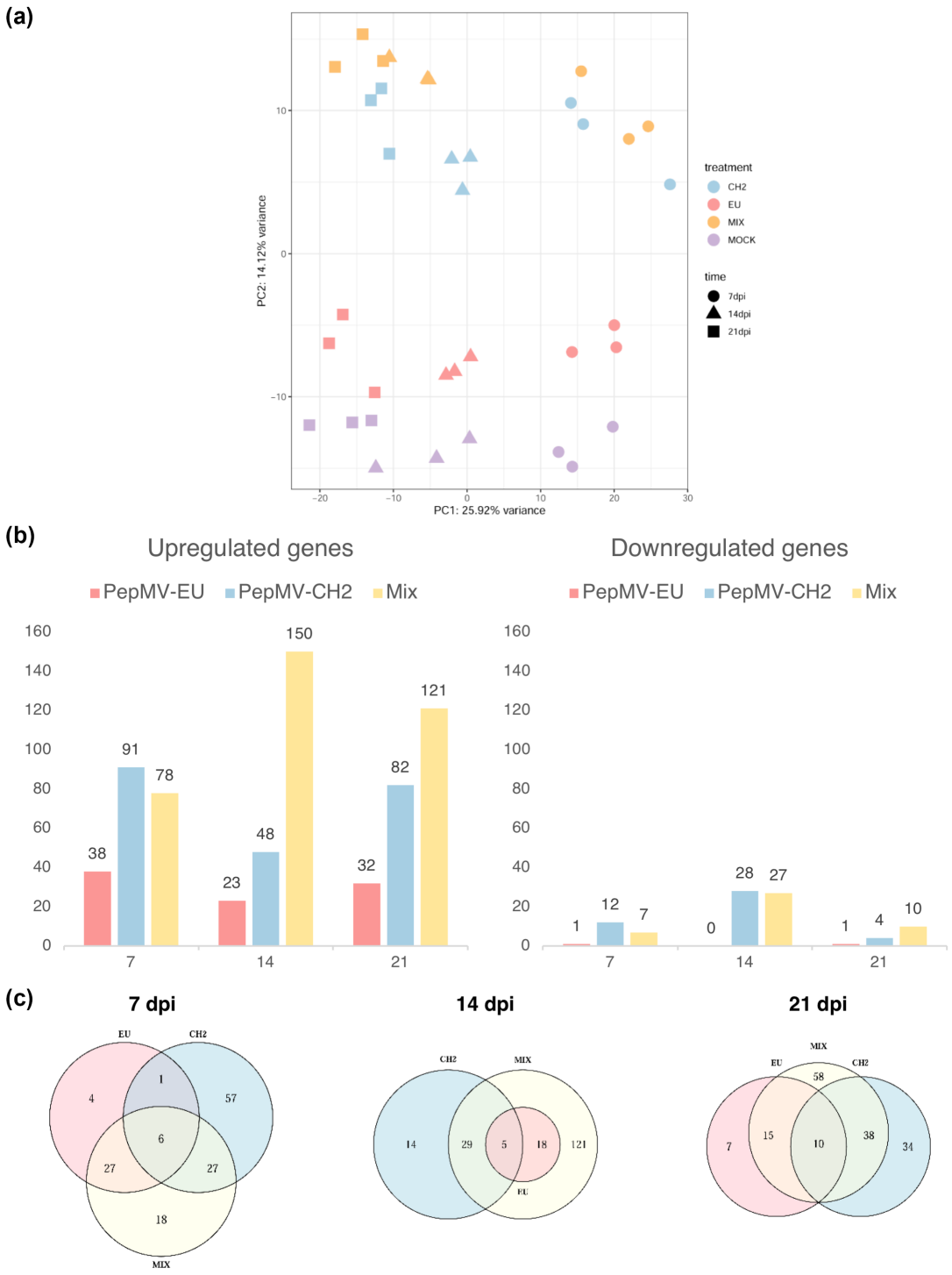

FIGURE 2 Exploratory analysis of transcriptomic data. (a) Principal component analysis of all replicates from the different treatments (colours) at each time postinfection (shapes; dpi, days postinoculation). (b) Number of up- and down-regulated genes in each type of infection with respect to the mock treatment at each time. (c) Venn diagrams of the up-regulated genes at each time, showing the specific and shared genes between treatments.

versus PepMV-CH2 and mixed infections (Figure 2c), whereas at 14 and 21 dpi there was a larger number of up-regulated genes specific for the mixed infection that were not shared with the single infections (121 and 58, respectively) (Figure 2c). In general, PepMV-CH2 and mixed infections had stronger effects on the host transcriptome than PepMV-EU alone, in agreement with the data distribution in the principal component analysis, where the PepMV-EU treatment appeared close to the mock treatment and PepMV-CH2 close to the mixed infections one (Figure 2a), and this is also in agreement with the virus titres in the plants (Figure 1).

2.3 | Single infections with each of the viral strains differentially modulate the tomato transcriptome

To study the expression profile associated with each viral strain, we compared the transcriptomes of singly-infected plants. We found 7, 5, and 10 up-regulated genes shared between infections with PepMV-EU and -CH2 at 7, 14, and 21 dpi, respectively (Figure 2c), with some of them associated with the plant's general stress response. At 7 dpi, we found 118 DEGs during either virus infection, 49 of them were up-regulated by PepMV-EU and 69 by PepMV-CH2 (Table S2). Among the genes up-regulated by PepMV-EU, those with nuclear functions (i.e., transcription factors and DNA repair functions) and stress-responsive genes (i.e., genes related to phytohormone levels, involved in protection against oxidative damage or associated with plant defence) seemed to be over-represented (Table S2). In the case of up-regulated genes in PepMV-CH2 compared to PepMV-EU infections, we mainly found genes involved in the plant stress and defence responses (e.g., NBS-type resistance protein RGC2), and an important proportion of genes involved in lipid metabolism (e.g., lipase, lipid A export ATP-binding/permease protein msbA, sterol reductase, among others) (Table S2). At 14 dpi, 44 DEGs were found (Table S3): 17 up-regulated in PepMV-EU and 27 in PepMV-CH2. Finally, at 21 dpi, 52 DEGs were found (Table S4), 16 of which were up-regulated in the case of PepMV-EU and 36 in the case of PepMV-CH2. Most of the genes up-regulated at 14 and 21 dpi were associated with the same functions as those identified at 7 dpi (Tables S3 and S4). In general terms, the number of DEGs was larger at 7 dpi than at the other sampling times, indicating that stronger transcriptomic alterations occur at early infection times. Another trend that clearly emerged was that each of the viral strains modulated the host transcriptome differentially.

2.4 | Single and mixed infections cause similar transcriptomic alterations at early infection times, but differ at later times

We next tested the hypothesis that mixed infections cause host transcriptome perturbations different from the sum of perturbations caused by single infections. For this we compared DEGs between mixed infections and the sum of single infections. No DEGs were found at 7 dpi, 112 DEGs were found at 14 dpi, and 15 at 21 dpi. Of the 112 DEGs found at 14 dpi (Table S5), 20 genes were up-regulated in single infections (e.g., a metascapase, a glucanase, and three reductase-encoding genes) with respect to mixed infections, and 92 were up-regulated in mixed infections with respect to single infections, 22 of them related to electron transfer chains (e.g., cytochrome P450, photosystems I and II, and NADPH quinone-encoding genes), six related to the plant's stress response, and seven genes of the family encoding ribulose bisphosphate carboxylase. Finally, at 21 dpi, 15 genes were up-regulated in mixed infections compared with single infections (Table S6), for example genes encoding a glutathione S-transferase and an NBS-LRR class disease resistance protein. In conclusion, at 7 dpi, when the larger number of genes was up-regulated, mixed infections caused transcriptomic alterations that seemed to be the sum of those caused by single infections; in contrast, at 14 and 21 dpi, mixed infections induced host transcriptome changes that were different from the sum of alterations caused by each single infection.

2.5 | Up-regulated genes along the progress of infection

The above data indicate, among other things, that the sampling time along the progress of the infection is a crucial determinant of the host transcriptome during virus infections. To study this aspect in more detail, gene expression levels were estimated for each time and treatment using the DESeq2 R package. Expressed genes were considered those with FPKM values >1, and these were the genes used for further analyses. Then, genes that were up-regulated in a time-specific manner were identified for each type of infection (Figure 3), defining time-specific genes as those that had at least a 2-fold or more increase in expression at one time compared to the others. In PepMV-EU single infection, we found 184 time-specific genes up-regulated at 7 dpi, 15 at 14 dpi, and 110 at 21 dpi. In the case of PepMV-CH2 single infection, 222 genes were up-regulated at 7 dpi, seven at 14 dpi, and 147 at 21 dpi. In the mixed infection, 355 up-regulated genes were found at 7 dpi, 49 at 14 dpi, and 33 at 21 dpi (Figure 3). A GO enrichment analysis showed that in the PepMV-EU single infection, the 7 dpi time was enriched in genes related to "DNA binding" and the 21 dpi time in genes related to "plastid", "plasma membrane light-harvesting complex", "carbon fixation", "cell wall", and "sinapoylglucose-malate O-sinapoyltransferase activity" (Figure 3). No enriched GO terms were found at 14 dpi. For PepMV-CH2, no enriched GO terms were found at 7 or 14 dpi, and the 21 dpi time was enriched in genes related to "plastid", "carbon fixation", and "plasma membrane light-harvesting complex" (Figure 3). For mixed infections, the 7 dpi time was enriched in genes related to "microtubule-based movement", "nucleus", "microtubule binding", "DNA binding", and "cyclin-dependent protein serine/threonine kinase regulator activity" (Figure 3). No enriched GO terms were found at 14 or 21 dpi (Figure 3). In general, all the treatments showed more specifically up-regulated genes at 7 dpi than at the other sampling times, which again indicates a more pronounced host transcriptomic perturbation at early PepMV infection times.

2.6 | A search for host genes potentially involved in the PepMV-EU versus PepMV-CH2 antagonism

We next tested the hypothesis that PepMV-EU, in either single or mixed infections, deregulates host gene expression in such a way that PepMV accumulation is repressed. We thus focused on comparing genes up-regulated by PepMV-EU (in single or mixed infection) with genes up-regulated by PepMV-CH2 in single infection. We used

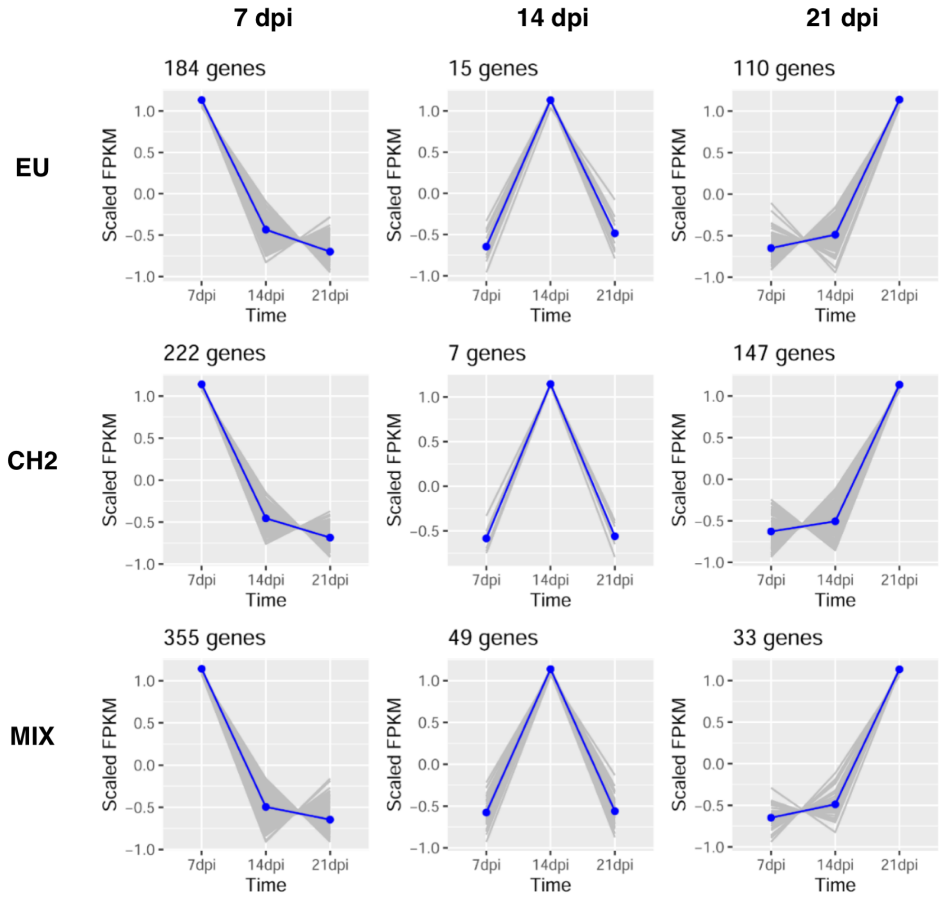

Treatment	Time	GO term	Description
EU	7	GO:0003677	DNA binding
	21	GO:0009536	plastid
		GO:0030077	plasma membrane light-harvesting complex
		GO:0015977	carbon fixation
		GO:0005618	cell wall
		GO:0016754	sinapoylglucose-malate O-sinapoyltransferase activity
CH2	21	GO:0009536	plastid
		GO:0015977	carbon fixation
Mix	7	GO:0007018	microtubule-based movement
		GO:0005634	nucleus
		GO:0008017	microtubule binding
		GO:0003677	DNA binding
		GO:0016538	cyclin-dependent protein serine/threonine kinase regulator activity

FIGURE 3 Time-specific genes for each type of infection. Expression patterns of genes up-regulated in a time-specific manner are shown for each treatment (EU, CH2, and mix). On top of each graphic, the total number of specifically up-regulated genes is indicated, on the *x* axis the time postinoculation and on the *y* axis the scaled fragments per kilobase per million mapped reads (FPKM) values. The table on the bottom shows the enriched Gene Ontology (GO) terms for each treatment and time (dpi, days postinoculation).

the same methodology as in the previous section; a significant proportion of the up-regulated genes was shared by all sampling times, with just 31, 20, and 15 being specific for the comparisons at 7, 14, and 21 dpi, respectively (Figure 4). We then reasoned that whatever was repressing PepMV-CH2 accumulation in mixed infections at 7 dpi becomes less active at 14 dpi, as PepMV-CH2 accumulation in mixed infections starts to return to single infection levels by this time after inoculation (Figure 1). We found 15 genes specifically up-regulated at 7 dpi, among which we found genes encoding a zinc finger family protein, an auxin-induced SAUR-like protein, a tyrosine aminotransferase, a UDP-glucosyltransferase, a transcription anti-termination protein, and Argonaute 2a (*AGO2a*) (Figure 4). Following

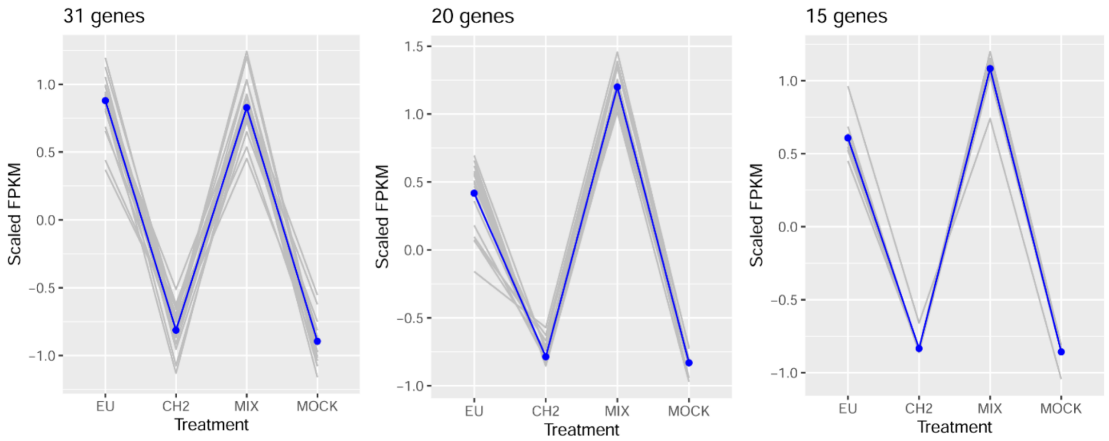

7 dpi	14 dpi	21 dpi
β-1,3-glucanase	**β-1,3-glucanase**	Programmed cell death 7
26S proteasome non-ATPase regulatory subunit	Programmed cell death 7	Fanconi anemia group D2 protein
Unknown protein	Fanconi anemia group D2 protein	Translation initiation factor eIF-2B subunit epsilon
Programmed cell death 7	Translation initiation factor eIF-2B subunit epsilon	Dipeptidyl peptidase IV-like protein
Fanconi anemia group D2 protein	Dipeptidyl peptidase IV-like protein	ATP-binding cassette (ABC) transporter 17
Translation initiation factor eIF-2B subunit epsilon	ATP-binding cassette (ABC) transporter 17	Unknown protein
Unknown protein	Unknown protein	Xanthoxin dehydrogenase
Argonaute 2a	Xanthoxin dehydrogenase	DNA repair protein Rad50
Cathepsin B-like cysteine proteinase	DNA repair protein Rad50	Epoxide hydrolase
Dipeptidyl peptidase IV-like protein	Epoxide hydrolase	Zinc finger family protein
ATP-binding cassette (ABC) transporter 17	Zinc finger family protein	Calmodulin-binding protein
Unknown protein	**NBS-LRR class disease resistance protein**	MYB transcription factor
Auxin-induced SAUR-like protein	**Subtilisin-like protease**	Inositol 1 4 5-trisphosphate 5-phosphatase-like protein
Xanthoxin dehydrogenase	Calmodulin-binding protein	UDP-glucuronosyltransferase
DNA repair protein Rad50	MYB transcription factor	Avr9/Cf-9 rapidly elicited protein 65
Epoxide hydrolase	Inositol 1 4 5-trisphosphate 5-phosphatase-like protein	
Unknown protein	**Sigma factor binding protein 1**	
Zinc finger family protein	**Cytochrome P450**	
Unknown protein	**PAR-1c protein**	
Zinc finger family protein	**Unknown protein**	
NBS-LRR class disease resistance protein		
Unknown protein		
Subtilisin-like protease		
Calmodulin-binding protein		
Transcription antitermination protein nusG		
Protein RDM1		
Unknown protein		
Tyrosine aminotransferase		
MYB transcription factor		
Inositol 1 4 5-trisphosphate 5-phosphatase-like protein		
UDP-glucosyltransferase family 1 protein		

FIGURE 4 Genes specifically up-regulated by the PepMV-EU infection. Expression patterns of genes that were highly expressed during PepMV-EU infections (single and mixed) and not during PepMV-CH2 or mock treatments are shown. On top of each graphic, the total number of genes is indicated, on the *x* axis the time (dpi, days postinoculation) and on the *y* axis the scaled fragments per kilobase per million mapped reads (FPKM) values. The table on the bottom shows the annotated function for each gene.

the same reasoning, we next looked at genes up-regulated at 14 dpi compared to 21 dpi, as PepMV-CH2 accumulation in mixed infections recovers to single infection levels from 14 to 21 dpi. We thus found seven specifically up-regulated genes, among them genes encoding a subtilisin protease, a β-1,3 glucanase, a cytochrome P450, and a NBS-LRR class disease resistance protein (Figure 4). Given the identification of *AGO2a* in the list above, we decided to analyse whether other genes from the antiviral silencing pathway were co-regulated with *AGO2a*. A clustering analysis and a heatmap of the scaled FPKMs at 7 dpi of the different AGO, DCL, and RDR protein expressing genes (FPKM >1) in tomato were performed (Figure 5a). The clustering analysis provided three clear groups depending on

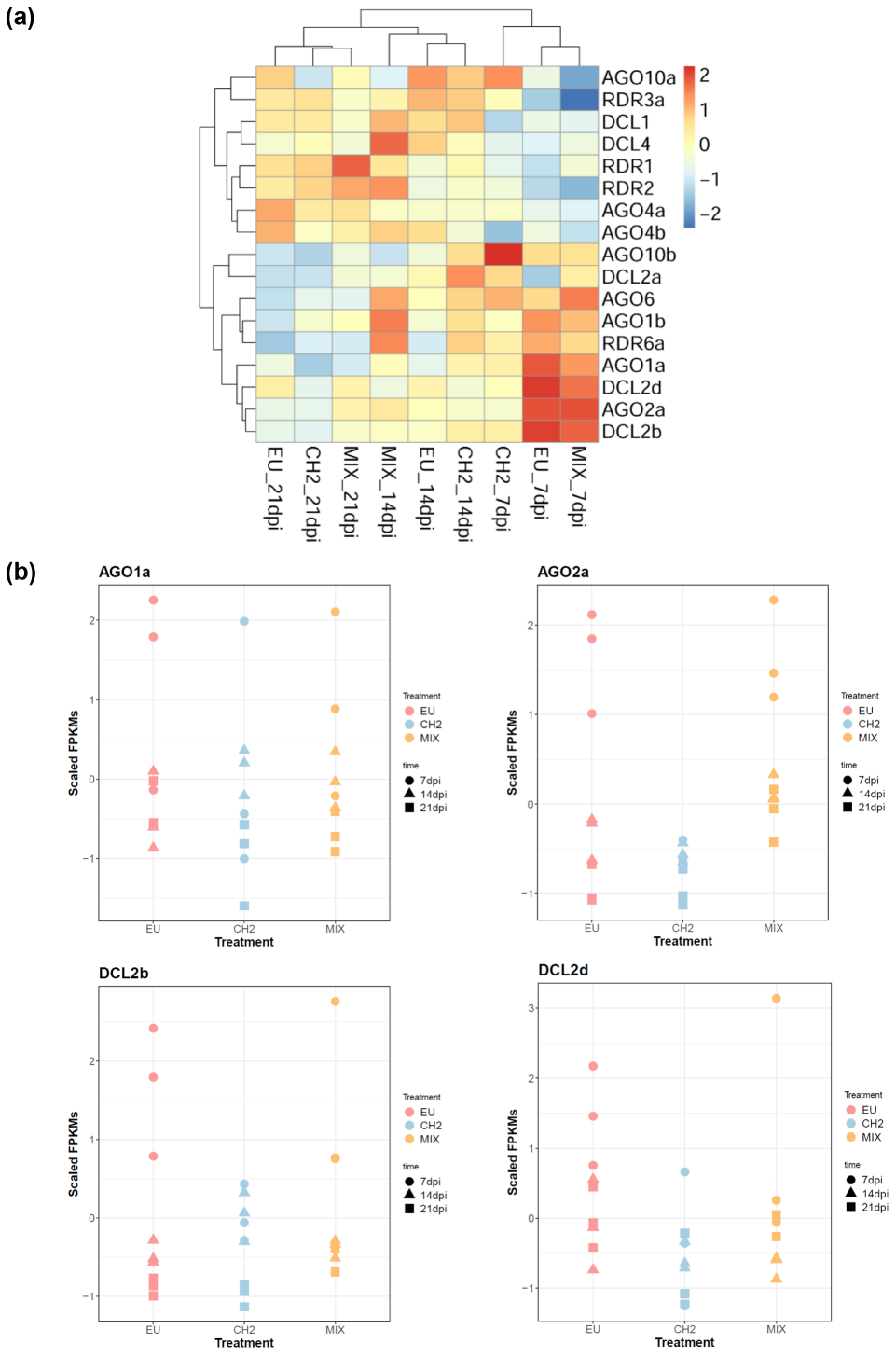

FIGURE 5 Involvement of RNA silencing genes in PepMV infection. (a) Heatmap of the genes involved in the antiviral silencing that are expressed (fragments per kilobase per million mapped reads; FPKMs >1) in tomato plants. Scaled FPKM values were used as input of the heatmap and are represented by colours. Red means higher expression and blue lower. (b) Values of scaled FPKMs for the four main determinant genes of the clustering between PepMV-EU and mixed versus PepMV-CH2 infection at 7 days postinoculation. Scaled FPKMs are shown for each treatment and time for *AGO1a*, *AGO2a* (on top), *DCL2b*, and *DCL2d* (on the bottom). Times postinoculation are shown in different colours and treatments with different shapes.

the sampling time, although at 7 dpi the PepMV-EU and mix infections grouped together and were quite different to PepMV-CH2 (Figure 5a, see vertical clustering). *AGO1a*, *DCL2d*, *AGO2a*, and *DCL2b* appeared to be principal determinants of this differentiation (Figure 5a, see horizontal clustering). Statistically significant differences were found only for *AGO2a* scaled FPKMs at 7 dpi, with high expression levels at 7 dpi in PepMV-EU and mixed infections, and not in PepMV-CH2 single infection ($F = 21.98$, $p < 0.01$) (Figure 5b).

2.7 | *AGO2a* plays a role in PepMV infection, differentially responding to the PepMV strains, both in tomato and in *N. benthamiana*

To validate the *AGO2a* results above, a relative reverse transcription-quantitative PCR (RT-qPCR) was performed on the same set of tomato samples (Figure 6a). At 7 dpi, significant differences were found in *AGO2a* expression between mock and PepMV-EU ($F = 12.46$, $p = 0.024$), mock and mix ($F = 19.82$, $p = 0.011$), PepMV-CH2 and PepMV-EU ($F = 13.97$, $p = 0.020$), and PepMV-CH2 and mix ($F = 45.19$, $p = 0.003$) (Figure 6a). In contrast, no differences were found between mock and PepMV-CH2 single infection, or PepMV-EU and mixed-infected plants. No significant differences in *AGO2a* expression were found between treatments at 14 or 21 dpi (Figure 6a). These results confirm the RNA-Seq data, showing the up-regulation of *AGO2a* in plants infected with PepMV-EU (in single or mixed infections) in comparison with plants infected with PepMV-CH2 or the mock treatment at early infection times. Therefore, *AGO2a* seems to play a role in PepMV infections of tomato plants depending on the infecting strain.

We next took advantage of the amenability of *N. benthamiana* as a virus model host. We first analysed *AGO2* expression in mock and PepMV-infected *N. benthamiana* plants by RT-qPCR (Figure 6b). Significant differences were found at 7 dpi between mock plants and PepMV-EU ($F = 269.76$, $p < 0.001$), PepMV-CH2 ($F = 17.37$, $p = 0.014$), and PepMV-EU + PepMV-CH2 ($F = 27.42$, $p = 0.006$) infected plants (Figure 6b). At 14 dpi, significant differences were found between mixed-infected plants and the other treatments, mock ($F = 23.88$, $p = 0.008$), PepMV-EU single infection ($F = 21.96$, $p = 0.009$), and PepMV-CH2 single infection ($F = 10.08$, $p = 0.034$). No significant differences were found at 21 dpi between treatments (Figure 6b). However, the pattern of *AGO2* expression in *N. benthamiana* did not fully recapitulate that in tomato: we found significant differences at 7 dpi between PepMV-CH2 single infected and mock plants, and also a sharp up-regulation at 14 dpi in mixed infection. We then quantified PepMV accumulation in single and mixed infections in *N. benthamiana* plants. PepMV-EU and PepMV-CH2 accumulation was similar in *N. benthamiana* wild-type plants (Figure 7) compared to tomato MicroTom plants (Figure 1), showing no differences between single and mixed infections at any time (7, 14, or 21 dpi) in the case of PepMV-EU (Figure 7a), and significant differences between single and mixed infections at 7 dpi ($F = 2347.89$, $p < 0.001$) in the case of PepMV-CH2 (Figure 7b). *N. benthamiana* plants knocked out for *AGO2* have been produced, and their inoculation with a diverse set of viruses, including potato virus X (PVX) (also a potexvirus, like PepMV), showed the enhanced susceptibility of the *ago2* mutant (Ludman et al., 2017). We thus decided to use this mutant to further study the role of *AGO2* in PepMV infections. An experiment with the same layout as before was carried out with mutant plants, again sampling at 7, 14, and 21 dpi. The symptomatology was evaluated in *ago2* versus wild-type *N. benthamiana* plants. In general, symptoms were more severe in *ago2* plants, showing dwarfism, leaf bubbling, chlorosis, and yellowing mosaics on leaves (Figure S1). The PepMV accumulation in these plants was much higher than in wild-type *N. benthamiana* plants ($F = 15.10$, $p < 0.001$), up to 30 times higher in the case of PepMV-EU and up to five times higher in the case of PepMV-CH2, suggesting a more important role of *AGO2* in repressing PepMV-EU than for PepMV-CH2. The accumulation trends were similar to those found in wild-type *N. benthamiana* and tomato plants, with no significant differences between single PepMV-EU and mixed infections at any of the tested times (Figure 7a). For PepMV-CH2, significant differences were found between single and mixed infections at 7 dpi ($F = 95.80$, $p = 0.001$) and at 21 dpi ($F = 81.23$, $p = 0.001$) (Figure 7b). In conclusion, our data showed that *AGO2* plays a clear role in PepMV infection, but it does not seem to be a direct or the only responsible actor for the PepMV-EU versus PepMV-CH2 antagonism, at least in *N. benthamiana*.

3 | DISCUSSION

Although mixed viral infections are common in nature, there is scant knowledge on the effect that they can have on the host transcriptome (Seo et al., 2018), particularly for the case of mixed infections of two strains of the same virus. PepMV is an important pathogen in tomato crops that causes significant economic losses worldwide. Mixed infections of isolates belonging to two strains of PepMV, EU and CH2, are frequent in crops, and although their eco-evolutive interactions have been extensively studied (Alcaide et al., 2020, 2021; Alcaide & Aranda, 2021; Gómez et al., 2009), the host transcriptome responses in both single and mixed infections have not been documented, despite their interest to understand the role of the host in the mediation of the asymmetric antagonism shown between isolates of both strains. A previous tomato transcriptome profiling after PepMV infection was performed using a GeneChip array that contained probe sets to interrogate over 22,000 tomato transcripts. The authors identified DEGs in infections with a mild and an aggressive isolate of the same strain, CH2 (Hanssen et al., 2011), finding that PepMV infection was associated with a transient repression of the primary metabolism that was also influenced by the time of infection. In our study, we first compared DEGs between PepMV-EU and PepMV-CH2 in single infections, finding that most of the shared up-regulated genes for both viruses were mainly related to the plant's stress responses. However, most of the genes that were up-regulated during the PepMV-EU single infection were different to those up-regulated by PepMV-CH2, even if they were related in both cases to the plant's stress response. In addition, in the case of PepMV-CH2, genes encoding enzymes participating in lipid metabolism were altered, which could also be related to plant defence (Kachroo & Kachroo, 2009; Wang, 2014) or with the membrane remodelling needed for efficient viral replication (Laliberté & Zheng, 2014; Nagy & Feng, 2021). In the case of PepMV-EU, genes related with phytohormone levels, which are involved in plant defence (García-Andrade et al., 2020; Loake & Grant, 2007), were also up-regulated. Thus, although both strains triggered host defence responses, they appeared to be activating different plant defence

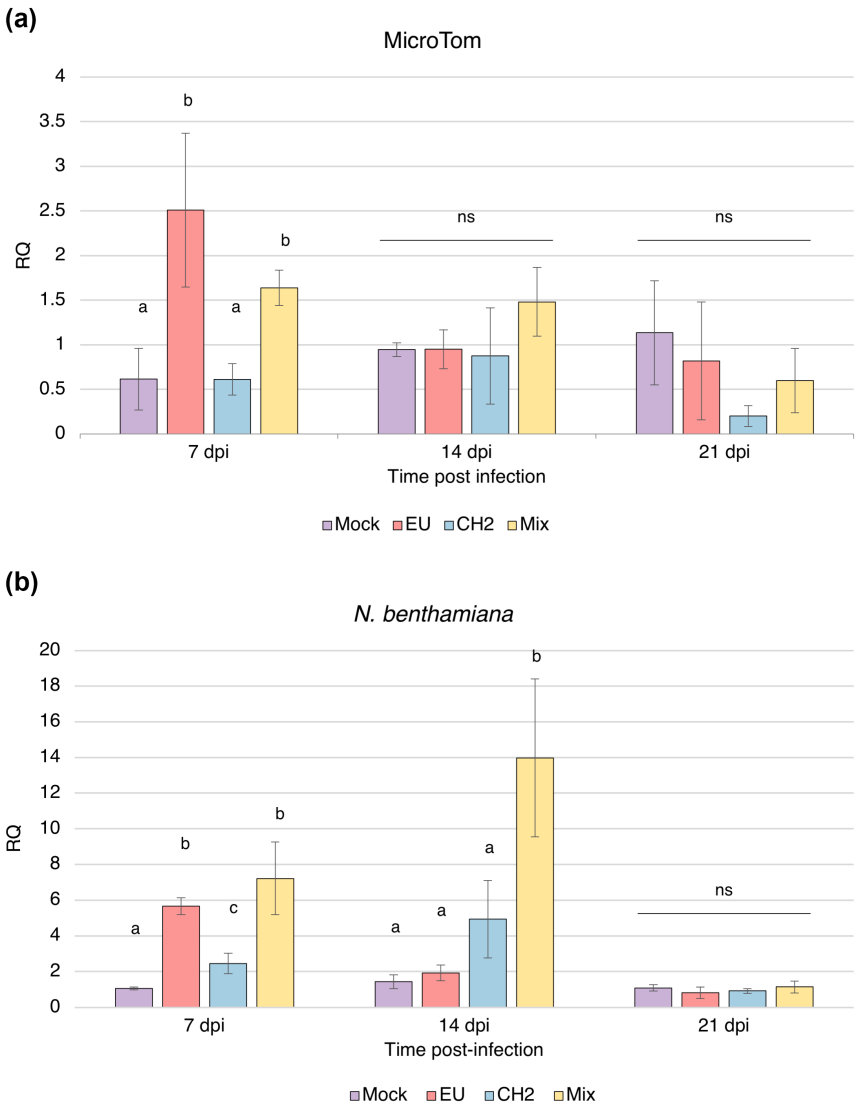

FIGURE 6 *AGO2a* expression in tomato and *Nicotiana benthamiana* plants. (a) Relative expression of *AGO2a* in MicroTom mock, PepMV-EU, PepMV-CH2, and mixed-infected plants at different times (dpi, days postinoculation). (b) Relative expression of *AGO2* in *N. benthamiana* mock, PepMV-EU, PepMV-CH2, and mixed-infected plants at different times postinoculation. *AGO2* expression was determined for each time point by relative reverse transcription-quantitative PCR using *EF1α* and *PP2A* as endogenous controls for MicroTom and *N. benthamiana* assays, respectively. Each treatment included three biological replicates. Each bar represents the mean and its standard deviation. Different lower case letters (a, b, or c) indicate treatments that are significantly different; ns = not significant.

pathways. A differential response to two strains of the same virus has also been described for turnip mosaic virus (TuMV), observing that concomitant with inducing a different symptomatology in *A. thaliana*, they differentially regulated key genes involved in the senescence process (Manacorda et al., 2013). Indeed, most of the studies comparing infections with different virus isolates were primarily motivated and focused on differences on symptomatology, associating symptomatology with differential host transcriptomic responses (Geng et al., 2017; Hanssen et al., 2011; Ramírez-Pool et al., 2022; Zanardo et al., 2019). The above studies showed a trend correlating viral accumulation with the extent of transcriptomic perturbations in the host (Hillung et al., 2012; Zanardo et al., 2019), which agrees with our data, which shows stronger transcriptomic alterations for PepMV-CH2 than for PepMV-EU.

When we compared the host response to single and mixed infections, we found no differences at 7 dpi. However, large differences were found at 14 dpi, as evidenced by the up-regulation of genes involved in electron transfer chains, stress response, and the Benson–Calvin cycle in mixed infections, with similar alterations described for other viruses (Zanardo et al., 2019). In both cases, comparing PepMV-EU versus PepMV-CH2 single infections, and single versus mixed infections, we found that the time postinfection largely determined the host transcriptome status, reinforcing the idea that the transcriptome is a snapshot of a specific moment of the life cycle of the plant and of the course of infection. Thus, many of the transcriptomic analyses studied the plant response to viral infections at different time points (Zanardo et al., 2019), finding, for example in the case of rice stripe virus, a shift between up- and down-regulated genes through time (Sun et al., 2016). In the case of PepMV, we found stronger transcriptomic remodelling at early times postinfection, which also agrees with data from Hanssen et al. (2011). At 7 dpi, plants singly infected with PepMV-EU or PepMV-CH2 were enriched in transcripts encoding histones and transcription factors, but plants singly infected with PepMV-CH2 were also enriched in transcripts encoding kinases and genes involved in lipid metabolism. Mixed-infected plants were enriched in transcripts encoding histones, transcription factors, kinases, and microtubule-related proteins. In general, PepMV infection altered the expression of histones and transcription factors that can be involved in the biotic stress response of plants (Amorim et al., 2016; Ramirez-Prado

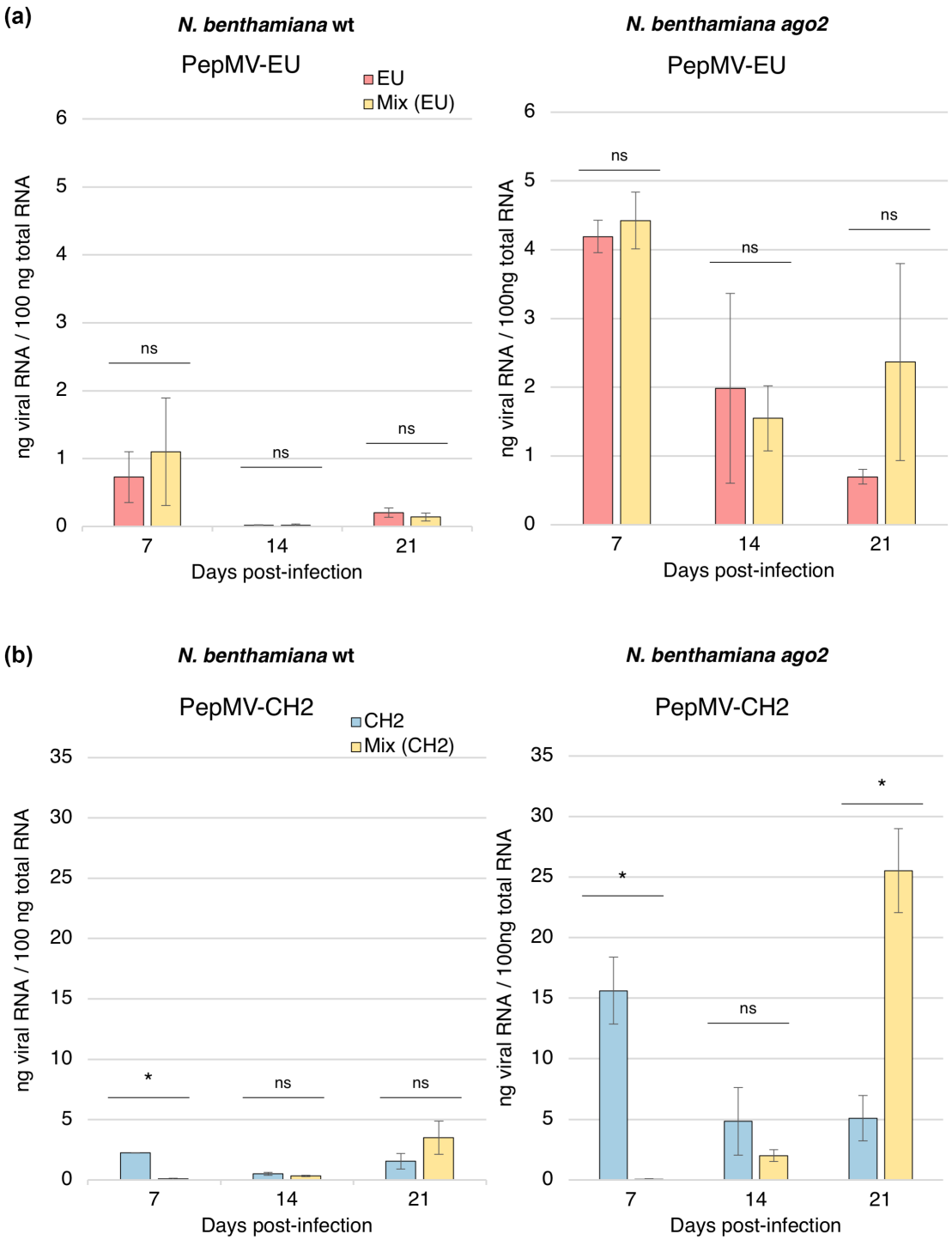

FIGURE 7 PepMV accumulation in *Nicotiana benthamiana* plants. (a) Accumulation of PepMV-EU in single (red) and mixed (orange) infections at different times postinoculation in wild-type (wt, left panel) and in *ago2* (right panel) *N. benthamiana* plants. (b) Accumulation of PepMV-CH2 in single (blue) and mixed (orange) infections at different times postinoculation in wild-type (left panel) and in *ago2* (right panel) *N. benthamiana* plants. Virus accumulation was determined by absolute reverse transcription-quantitative PCR and shown as nanograms of viral RNA/100 ng total RNA. Each treatment included three biological replicates. Each bar represents the mean and its standard deviation. Asterisks show significance level (*$p < 0.05$; ns = not significant).

et al., 2018). PepMV-CH2 infection also seemed to up-regulate the signalling transduction pathway. However, an abundant number of genes related with microtubules were found in mixed-infected plants. Microtubules are important for virus movement and the formation of viral replication complexes (Boyko et al., 2000; Niehl et al., 2013), although the reason behind their over-representation only in mixed infections is unknown. Only a few 14 dpi-specific up-regulated genes were found, with some of them related to the

expression of phytohormones. Finally, at 21 dpi, many genes related with carbon fixation and plasma membrane light-harvesting complex were up-regulated in PepMV-EU and PepMV-CH2 single infections. The deregulation of genes related with photosynthesis associated with virus infection has been widely described, usually related to the type of symptomatology produced in the host (Zanardo et al., 2019). Although plants infected with the PepMV isolates used in this work showed very mild symptoms at late stages postinfection, at early times postinfection leaf chlorosis could be observed (Figure S1). Therefore, it could be that genes related to photosynthesis were up-regulated in association with symptom recovery at 21 dpi. All these results show the importance of taking into consideration the sampling time during viral infections, which can help to determine the different stages that genes can go through during the progress of infection.

RNA silencing is a conserved antiviral mechanism that is expected to be deregulated during viral infections. Thus, we studied the expression patterns of genes encoding different proteins involved in the RNA silencing pathway during PepMV infection. We found that *AGO1a*, *AGO2a*, *DCL2b*, and *DCL2d* were the main genes that determined the clustering of PepMV-EU and mixed infections versus PepMV-CH2 infections at early infection times (Figure 5), pointing towards a differential activation of these RNA silencing genes by both viruses. One of the aims of our work was to identify host genes involved in the asymmetric antagonism observed between PepMV-EU and PepMV-CH2; therefore, we decided to focus on the genes up-regulated by PepMV-EU but not by PepMV-CH2. On that list, for example, we found a UDP-glucosyltransferase, which may play a role in plant resistance to virus infections in plants (Matros & Mock, 2004). However, a particularly interesting finding was the discovery of *AGO2a* on the list (Figure 4), prompting us to hypothesize that AGO2a could be directly responsible for the asymmetric antagonism in mixed infections, with its expression being up-regulated by PepMV-EU but not by PepMV-CH2, leading to PepMV repression in PepMV-EU single infection and also in mixed infections, where it would target any PepMV isolate. To test this hypothesis, we used *ago2 N. benthamiana* plants. We first showed that the asymmetric antagonism observed in tomato also took place in *N. benthamiana*. However, our results showed that, despite the higher accumulation of PepMV-EU and PepMV-CH2 in *ago2 N. benthamiana* plants with respect to wild-type plants, the asymmetric antagonism pattern remained as in wild-type plants. Therefore, it appears that *AGO2* indeed plays an important role in the antiviral defence against PepMV, as it was described before for PVX and other RNA viruses such as TuMV and turnip crinkle virus (Kamitani et al., 2016; Ludman et al., 2017), but it does not seem to be a primary factor that determines PepMV antagonism. As some AGO and DCL proteins have redundant functions, it may be that, in the absence of AGO2, other proteins assume its role. Also, AGO2 may not be the only factor involved in the asymmetric antagonism observed, and there may be another set of factors that act in a coordinated manner, for example other AGO or DCL proteins, and the absence of only one of these factors may not be sufficient to unveil its role. The mechanism by which PepMV-CH2 maintains the expression of *AGO2* unperturbed during infection is also unknown. Two potexvirus proteins have been described as silencing suppressors, TGB1 and CP. It may be possible that the silencing suppressors of PepMV-CH2 are more efficient than those of PepMV-EU, which could explain why PepMV-CH2 isolates have a higher fitness than PepMV-EU isolates (Alcaide et al., 2020), resulting in the displacement of the latter in the field (Gómez-Aix et al., 2019). Also, it could explain why coinfections are maintained, with PepMV-EU activating the RNA silencing machinery and competing against PepMV-CH2 despite the higher fitness of the latter in single infections. This agrees with our previous study, in which we demonstrated that whether mixed infections are simultaneous or delayed is crucial for the asymmetric antagonism (Alcaide & Aranda, 2021), as the data presented here suggest that *AGO2* up-regulation depends on the time after inoculation. Further research is needed to better understand the possible implications of other proteins involved in the antiviral RNA silencing response on the asymmetric antagonism, including AGOs and DCLs, but also the silencing suppressors of PepMV-EU and PepMV-CH2.

4 | EXPERIMENTAL PROCEDURES

4.1 | Plant growth and virus inoculation

For transcriptome analyses, tomato plants (cv. MicroTom) were mechanically inoculated with PepMV-EU, PepMV-CH2, or PepMV-EU + PepMV-CH2 in mixed infection, using 27 plants per treatment. For inoculations, purified virions (see below) of PepMV-Sp13 (EU type) (Aguilar et al., 2002) and PepMV-PS5 (CH2 type) (Gómez et al., 2009) diluted in 30 mM phosphate buffer were used. In the case of mixed infections, virions of both isolates were mixed in a 1:1 proportion at the same concentration (100 ng/μl). For the mock treatment, 30 mM phosphate buffer without virions was used. Plants were grown in a growth chamber with a 16/8 h photoperiod set at 24°C. At 7, 14, and 21 dpi, all the leaves, except for the inoculated ones, were collected from nine plants per treatment. The samples collected from three plants were pooled per treatment and time postinoculation, obtaining three pools of three plants for each treatment and time; each pool was considered a biological replicate.

A similar experiment was carried out using wild-type and *ago2 N. benthamiana* plants (Ludman et al., 2017), but in that case individual plants were used as biological replicates, collecting the material from three individual plants for each treatment and time point.

4.2 | Virion purification

Twenty *N. benthamiana* plants were agroinfiltrated with each agroinfectious clone, PepMV-Sp13 (PepMV-EU) (Aguilar et al., 2002), or PepMV-PS5 (PepMV-CH2) (Gómez et al., 2009) separately; 7 days after the inoculation, systemically infected leaves were collected to purify virions. For this, tissue was ground using

liquid N_2 and homogenized in 0.1 M Tris-citric buffer pH 8, 0.2% β-mercaptoethanol, 1% Triton X-100, and 10 mM sodium thioglycolate. Then, chloroform was added in a 1:4 proportion and after centrifugation (15,000 × *g* for 15 min), a 5% polyethylene glycol (PEG) 8000 precipitation was carried out, incubating it for 1 h. Finally, a series of low- (10,000 × *g*) and high- (82,000 × *g*) speed centrifugation steps was performed (AbouHaidar et al., 1998; Agirrezabala et al., 2015). Optical densities at 260 and 280 nm of the virion preparations were measured in a NanoDrop One (Thermo Fisher Scientific) and the concentrations estimated using 2.9 as the extinction coefficient (AbouHaidar et al., 1998). Virion preparations were stored at 4°C.

4.3 | RNA extraction and library construction

Samples were ground in liquid N_2 and mixed with TNA buffer (2% SDS, 0.1 M Tris-HCl pH 8, 10 mM EDTA pH 8) in a proportion of 4 ml/g of tissue to homogenize them. Afterwards, RNA was extracted using the NZY Total RNA Isolation kit (NZYTech) following the manufacturer's recommendations. The RNA concentration was normalized after a DNase I treatment (Sigma-Aldrich) and total RNA integrity was analysed using an Agilent Technologies 2100 Bioanalyzer. After performing quality control, all the samples were submitted to library construction using Illumina TruSeq stranded total RNA libraries with Ribo-Zero, and sequenced using an Illumina NovaSeq 6000 platform (Macrogen Inc.), returning 150 bases of paired-end reads.

4.4 | Viral quantification by RT-qPCR

After the DNase I treatment (Sigma-Aldrich) of total RNA samples, the virus accumulation was measured by RT-qPCR using One-step NZYSpeedy RT-qPCR Green Kit and ROX Plus (NZYTech) with specific primers for PepMV-EU (CE-2651 5′-CCCCAAGTGGACTGCGTTAC-3′ and CE-2652 5′-GCAGCATTGTCGTCATCAGT-3′) and PepMV-CH2 (CE-2816 5′-AACCCAAGGCTGCTGATAACA-3′ and CE-2817 5′-AAGCCGTGTGCATTAAGCAA-3′). Pure viral RNA was obtained from the virion preparations with a phenol-chloroform extraction, following the protocol described by AbouHaidar et al. (1998). The standard curve for absolute quantification was then prepared performing 1:10 serial dilutions of this pure viral RNA.

4.5 | Bioinformatics analyses

Quality control was performed on the raw data and on the filtered reads (see below) using FastQC (Andrews, 2014). Reads with an average quality (Phred) lower than 30, Illumina adapters, and low-quality nucleotides at the 5′ end were removed with Trimmomatic (Bolger et al., 2014). After a second quality control round, pairs were repaired with BBMap (www.sourceforege.net/projects/bbmap). Reads were then mapped using the MEM algorithm from the BWA software (Li & Durbin, 2009) against the reference genome of *Solanum lycopersicum* (SL2.5 release; http://solgenomics.net). Mapping quality was evaluated using Qualimap (García-Alcalde et al., 2012). The function feature Counts from the Rsubread R package (Liao et al., 2019) was used to count the number of reads mapping to each mRNA (v2.4 of gene annotations). DEGs were determined among all the treatments using the Bioconductor package DESeq2 (Anders & Huber, 2010; Love et al., 2014). In addition, read counts were normalized to fragments per kilobase per million mapped reads (FPKM) using DESeq2 to obtain the relative levels of expression. Then, the expressed genes were considered those genes with a FPKM value higher than 1 in at least one treatment. A principal component analysis was drawn using the prcomp function in R and heatmaps using the pheatmap R package. Time-specific genes were those for which the FPKM value in one time was at least 2-fold the value in the remaining times, as described by Feng et al. (2017). Similarly, PepMV-EU- and mixed infection-specific genes were those for which the FPKM value was at least 2-fold the value in PepMV-CH2 and mock treatments. Finally, the goseq R package (Young et al., 2010) was used to perform a Gene Ontology (GO) enrichment analysis and to determine over-represented categories with a p value ≤0.05. The Wallenius approximation was used to calculate the unbiased category enrichment scores.

4.6 | *AGO2* mRNA quantification by relative RT-qPCR

After RNA extraction and DNAse I treatment, RT-qPCR was performed to quantify the *AGO2* mRNA levels in tomato and *N. benthamiana* plants. Primers CE-3101 5′-AGTGGTAGTGGAGTTGCTAATG-3′ and CE-3102 5′-CAGAA GATTGAGGAGGAGA ACG-3′ were used for tomato, and primers CE-3139 5′-CATGACTTTGGGTTTGGAGTT G-3′ and CE-3140 5′-CGGAATGCCAAGACTGAGTAA-3′ for *N. benthamiana*. As the endogenous control we used the transcripts of the elongation factor 1-alpha (*EF1α*) and the Ser/Thr protein phosphatase 2A (*PP2A*) for tomato and *N. benthamiana*, respectively. Primers CE-1199 5′-GATTGGTGGTATTGGAACTGTC-3′ and CE-1200 5′-AGCTTCGTGGTGCATCTC-3′ were used in the case of *EF1α*, and CE-3032 5′-GACCCTGATGTTGATGTTCGCT-3′ and CE-3033 5′-GAGGGATTTGAAGAGAGATTT C-3′ in the case of *PP2A*.

4.7 | Statistical analyses

Statistical analyses were carried out using IBM SPSS Statistics v. 26 and Statgraphics. General linear models were used to determine differences in virus accumulation and *AGO2a* mRNA levels between treatments. Analyses of variance (ANOVAs) were performed to evaluate the differences between the scaled FPKMs of *AGO1a*, *AGO2a*, *DCL2b*, and *DCL2d* in the different treatments and times.

ACKNOWLEDGEMENTS

The authors would like to thank Mari Carmen Montesinos (CEBAS-CSIC) for her help preparing and growing plants, and Mario Fon (mariogfon@gmail.com) for editing the manuscript. We also thank József Burgyán (Agricultural Biotechnology Institute, Gödöllő, Hungary) and Juan José López Moya (CRAG-CSIC, Barcelona, Spain) for providing the seeds of the *ago2 N. benthamiana* mutant. We acknowledge financial support from the Spanish Ministry of Science and Innovation through grants RTI2018-097099-B-100 and FPU16/02569.

CONFLICT OF INTEREST

Authors declare no conflict of interest.

DATA AVAILABILITY STATEMENT

The data that support the findings of this study are available from the corresponding author upon reasonable request.

ORCID

Cristina Alcaide https://orcid.org/0000-0002-7482-9810
Livia Donaire https://orcid.org/0000-0002-5454-2994
Miguel A. Aranda https://orcid.org/0000-0002-0828-973X

REFERENCES

AbouHaidar, M.G., Xu, H. & Hefferon, K.L. (1998) Potexvirus isolation and RNA extraction. In: Foster, G.D. & Taylor, S.C. (Eds.) *Plant virology protocols: from virus isolation to transgenic resistance*, Vol. 81. Totowa, NJ: Humana Press, pp. 131–143.

Agirrezabala, X., Méndez-López, E., Lasso, G., Sánchez-Pina, M.A., Aranda, M. & Valle, M. (2015) The near-atomic cryoEM structure of a flexible filamentous plant virus shows homology of its coat protein with nucleoproteins of animal viruses. *eLife*, 4, e11795.

Aguilar, J.M., Hernández-Gallardo, M.D., Cenis, J.L., Lacasa, A. & Aranda, M.A. (2002) Complete sequence of the Pepino mosaic virus RNA genome. *Archives of Virology*, 147, 2009–2015.

Alcaide, C. & Aranda, M.A. (2021) Determinants of persistent patterns of Pepino mosaic virus mixed infections. *Frontiers in Microbiology*, 12, 694492.

Alcaide, C., Rabadán, M.P., Juárez, M. & Gómez, P. (2020) Long-term co-circulation of two strains of pepino mosaic virus in tomato crops and its effect on population genetic variability. *Phytopathology*, 110, 49–57.

Alcaide, C., Sardanyés, J., Elena, S.F. & Gómez, P. (2021) Increasing temperature alters the within-host competition of viral strains and influences virus genetic variability. *Virus Evolution*, 7, veab017.

Amorim, L., Santos, R., Neto, J., Guida-Santos, M., Crovella, S. & Benko-Iseppon, A. (2016) Transcription factors involved in plant resistance to pathogens. *Current Protein & Peptide Science*, 18, 335–351.

Anders, S. & Huber, W. (2010) Differential expression analysis for sequence count data. *Genome Biology*, 11, R106.

Andrews, S. (2014) *FastQC: a quality control tool for high throughput sequence data*. Available from: http://www.bioinformatics.babraham.ac.uk/projects/fastqc/ [Accessed 4th Oct 2021].

Baulcombe, D. (2004) RNA silencing in plants. *Nature*, 431, 356–363.

Bayne, E.H., Rakitina, D.V., Morozov, S.Y. & Baulcombe, D.C. (2005) Cell-to-cell movement of potato potexvirus X is dependent on suppression of RNA silencing. *The Plant Journal*, 44, 471–482.

Bednarek, R., David, M., Fuentes, S., Kreuze, J. & Fei, Z. (2021) Transcriptome analysis provides insights into the responses of sweet potato to sweet potato virus disease (SPVD). *Virus Research*, 295, 198293.

Bolger, A.M., Lohse, M. & Usadel, B. (2014) Trimmomatic: a flexible trimmer for illumina sequence data. *Bioinformatics*, 30, 2114–2120.

Boyko, V., Ferralli, J., Ashby, J., Schellenbaum, P. & Heinlein, M. (2000) Function of microtubules in intercellular transport of plant virus RNA. *Nature Cell Biology*, 2, 826–832.

Carbonell, A. & Carrington, J.C. (2015) Antiviral roles of plant ARGONAUTES. *Current Opinion in Plant Biology*, 27, 111–117.

Ding, S.-W. (2010) RNA-based antiviral immunity. *Nature Reviews Immunology*, 10, 632–644.

Ding, S.W. & Voinnet, O. (2007) Antiviral immunity directed by small RNAs. *Cell*, 130, 413–426.

Ding, T.B., Li, J., Chen, E.H., Niu, J.Z. & Chu, D. (2019) Transcriptome profiling of the whitefly *Bemisia tabaci* MED in response to single infection of *Tomato yellow leaf curl virus*, *Tomato chlorosis virus*, and their co-infection. *Frontiers in Physiology*, 10, 302.

Donaire, L., Barajas, D., Martínez-García, B., Martínez-Priego, L., Pagán, I. & Llave, C. (2008) Structural and genetic requirements for the biogenesis of tobacco rattle virus -derived small interfering RNAs. *Journal of Virology*, 82, 5167–5177.

Feng, N., Song, G., Guan, J., Chen, K., Jia, M., Huang, D. et al. (2017) Transcriptome profiling of wheat inflorescence development from spikelet initiation to floral patterning identified stage-specific regulatory genes. *Plant Physiology*, 174, 1779–1794.

García-Alcalde, F., Okonechnikov, K., Carbonell, J., Cruz, L.M., Götz, S., Tarazona, S. et al. (2012) Qualimap: evaluating next-generation sequencing alignment data. *Bioinformatics*, 28, 2678–2679.

García-Andrade, J., González, B., Gonzalez-Guzman, M., Rodriguez, P.L. & Vera, P. (2020) The role of ABA in plant immunity is mediated through the PYR1 receptor. *International Journal of Molecular Sciences*, 21, 5852.

Geng, C., Wang, H.Y., Liu, J., Yan, Z.Y., Tian, Y.P., Yuan, X.F. et al. (2017) Transcriptomic changes in *Nicotiana benthamiana* plants inoculated with the wild-type or an attenuated mutant of Tobacco vein banding mosaic virus. *Molecular Plant Pathology*, 18, 1175–1188.

Gómez, P., Sempere, R.N., Elena, S.F. & Aranda, M.A. (2009) Mixed infections of Pepino mosaic virus strains modulate the evolutionary dynamics of this emergent virus. *Journal of Virology*, 83, 12378–12387.

Gómez, P., Sempere, R. & Aranda, M.A. (2012) Pepino mosaic virus and tomato torrado virus: two emerging viruses affecting tomato crops in the Mediterranean Basin. *Advances in Virus Research*, 84, 505–532.

Gómez-Aix, C., Pascual, L., Cañizares, J., Sánchez-Pina, M.A. & Aranda, M.A. (2016) Transcriptomic profiling of Melon necrotic spot virus-infected melon plants revealed virus strain and plant cultivar-specific alterations. *BMC Genomics*, 17, 429.

Gómez-Aix, C., Alcaide, C., Agüero, J., Faize, M., Juárez, M., Díaz-Marrero, C.J. et al. (2019) Genetic diversity and population structure of Pepino mosaic virus in tomato crops of Spain and Morocco. *Annals of Applied Biology*, 174, 284–292.

Hanssen, I.M. & Thomma, B.P. (2010) Pepino mosaic virus: a successful pathogen that rapidly evolved from emerging to endemic in tomato crops. *Molecular Plant Pathology*, 11, 179–189.

Hanssen, I.M., Paeleman, A., Wittemans, L., Goen, K., Lievens, B., Bragard, C. et al. (2008) Genetic characterization of Pepino mosaic virus isolates from Belgian greenhouse tomatoes reveals genetic recombination. *European Journal of Plant Pathology*, 121, 131–146.

Hanssen, I.M., van Esse, H.P., Ballester, A.R., Hogewoning, S.W., Parra, N.O., Paeleman, A. et al. (2011) Differential tomato transcriptomic responses induced by pepino mosaic virus isolates with differential aggressiveness. *Plant Physiology*, 156, 301–318.

Hillung, J., Cuevas, J.M. & Elena, S.F. (2012) Transcript profiling of different *Arabidopsis thaliana* ecotypes in response to tobacco etch potyvirus infection. *Frontiers in Microbiology*, 3, 229.

Jones, R.A.C. (2021) Global plant virus disease pandemics and epidemics. *Plants*, 10, 233.

Kachroo, A. & Kachroo, P. (2009) Fatty acid-derived signals in plant defense. *Annual Review of Phytopathology*, 47, 153–176.

Kamitani, M., Nagano, A.J., Honjo, M.N. & Kudoh, H. (2016) RNA-Seq reveals virus-virus and virus-plant interactions in nature. *FEMS Microbiology Ecology*, 92, fiw176.

Katsarou, K., Mitta, E., Bardani, E., Oulas, A., Dadami, E. & Kalantidis, K. (2019) DCL-suppressed *Nicotiana benthamiana* plants: valuable tools in research and biotechnology. *Molecular Plant Pathology*, 20, 432–446.

Laliberté, J.F. & Zheng, H. (2014) Viral manipulation of plant host membranes. *Annual Review of Virology*, 1, 237–259.

Li, H. & Durbin, R. (2009) Fast and accurate short read alignment with Burrows-Wheeler transform. *Bioinformatics*, 25, 1754–1760.

Li, K., Wu, G., Li, M., Ma, M., Du, J., Sun, M. et al. (2018) Transcriptome analysis of *Nicotiana benthamiana* infected by Tobacco curly shoot virus. *Virology Journal*, 15, 138.

Liao, Y., Smyth, G.K. & Shi, W. (2019) The R package Rsubread is easier, faster, cheaper and better for alignment and quantification of RNA sequencing reads. *Nucleic Acids Research*, 47, e47.

Ling, K.S., Li, R. & Bledsoe, M. (2013) Pepino mosaic virus genotype shift in North America and development of a loop-mediated isothermal amplification for rapid genotype identification. *Virology Journal*, 10, 117.

Linnik, O., Liesche, J., Tilsner, J. & Oparka, K.J. (2013) Unraveling the structure of viral replication complexes at super-resolution. *Frontiers in Plant Science*, 4, 6.

Liu, Q., Feng, Y. & Zhu, Z. (2009) Dicer-like (DCL) proteins in plants. *Functional & Integrative Genomics*, 9, 277–286.

Loake, G. & Grant, M. (2007) Salicylic acid in plant defence—the players and protagonists. *Current Opinion in Plant Biology*, 10, 466–472.

Love, M.I., Huber, W. & Anders, S. (2014) Moderated estimation of fold change and dispersion for RNA-seq data with DESeq2. *Genome Biology*, 15, 550.

Lu, J., Du, Z.X., Kong, J., Chen, L.N., Qiu, Y.H., Li, G.F. et al. (2012) Transcriptome analysis of *Nicotiana tabacum* infected by cucumber mosaic virus during systemic symptom development. *PLoS One*, 7, e43447.

Ludman, M., Burgyán, J. & Fátyol, K. (2017) Crispr/Cas9 mediated inactivation of Argonaute 2 reveals its differential involvement in antiviral responses. *Scientific Reports*, 7, 1010.

Manacorda, C.A., Mansilla, C., Debat, H.J., Zavallo, D., Sánchez, F., Ponz, F. et al. (2013) Salicylic acid determines differential senescence produced by two Turnip mosaic virus strains involving reactive oxygen species and early transcriptomic changes. *Molecular Plant-Microbe Interactions*, 26, 1486–1498.

Mathioudakis, M.M., Rodríguez-Moreno, L., Navarro Sempere, R., Aranda, M.A. & Livieratos, I. (2014) Multifaceted capsid proteins: multiple interactions suggest multiple roles for Pepino mosaic virus capsid protein. *Molecular Plant-Microbe Interactions*, 27, 1356–1369.

Matros, A. & Mock, H.P. (2004) Ectopic expression of a UDP-glucose: phenylpropanoid glucosyltransferase leads to increased resistance of transgenic tobacco plants against infection with potato virus Y. *Plant & Cell Physiology*, 45, 1185–1193.

Moreno, A.B. & López-Moya, J.J. (2020) When viruses play team sports: mixed infections in plants. *Phytopathology*, 110, 29–48.

Moreno-Perez, M.G., Pagan, I., Aragon-Caballero, L., Caceres, F., Fraile, A. & Garcia-Arenal, F. (2014) Ecological and genetic determinants of pepino mosaic virus emergence. *Journal of Virology*, 88, 3359–3368.

Morozov, S.Y. & Solovyev, A.G. (2003) Triple gene block: modular design of a multifunctional machine for plant virus movement. *Journal of General Virology*, 84, 1351–1366.

Nagy, P.D. & Feng, Z. (2021) Tombusviruses orchestrate the host endomembrane system to create elaborate membranous replication organelles. *Current Opinion in Virology*, 48, 30–41.

Niehl, A., Peña, E.J., Amari, K. & Heinlein, M. (2013) Microtubules in viral replication and transport. *The Plant Journal*, 75, 290–308.

Pagán, I., del Carmen Córdoba-Sellés, M., Martínez-Priego, L., Fraile, A., Malpica, J.M., Jordá, C. et al. (2006) Genetic structure of the population of Pepino mosaic virus infecting tomato crops in Spain. *Phytopathology*, 96, 274–279.

Pantaleo, V., Szittya, G. & Burgyán, J. (2007) Molecular bases of viral RNA targeting by viral small interfering RNA-programmed RISC. *Journal of Virology*, 81, 3797–3806.

Park, M.R., Jeong, R.D. & Kim, K.H. (2014) Understanding the intracellular trafficking and intercellular transport of potexviruses in their host plants. *Frontiers in Plant Science*, 5, 60.

Pumplin, N. & Voinnet, O. (2013) RNA silencing suppression by plant pathogens: defence, counter-defence and counter-counter-defence. *Nature Reviews Microbiology*, 11, 745–760.

Ramírez-Pool, J.A., Xoconostle-Cázares, B., Calderón-Pérez, B., Ibarra-Laclette, E., Villafán, E., Lira-Carmona, R. et al. (2022) Transcriptomic analysis of the host response to mild and severe CTV strains in naturally infected *Citrus sinensis* orchards. *International Journal of Molecular Sciences*, 23, 2435.

Ramirez-Prado, J.S., Piquerez, S.J.M., Bendahmane, A., Hirt, H., Raynaud, C. & Benhamed, M. (2018) Modify the histone to win the battle: chromatin dynamics in plant–pathogen interactions. *Frontiers in Plant Science*, 9, 355.

Sanjuán, R. (2021) The social life of viruses. *Annual Review of Virology*, 8, 183–199.

Sempere, R.N., Gómez, P., Truniger, V. & Aranda, M.A. (2011) Development of expression vectors based on pepino mosaic virus. *Plant Methods*, 7, 6.

Seo, J.K., Kim, M.K., Kwak, H.R., Choi, H.S., Nam, M., Choe, J. et al. (2018) Molecular dissection of distinct symptoms induced by tomato chlorosis virus and tomato yellow leaf curl virus based on comparative transcriptome analysis. *Virology*, 516, 1–20.

Solovyev, A.G., Kalinina, N.O. & Morozov, S.Y. (2012) Recent advances in research of plant virus movement mediated by triple gene block. *Frontiers in Plant Science*, 3, 276.

Sun, F., Fang, P., Li, J., Du, L., Lan, Y., Zhou, T. et al. (2016) RNA-seq-based digital gene expression analysis reveals modification of host defense responses by rice stripe virus during disease symptom development in Arabidopsis. *Virology Journal*, 13, 202.

Tilsner, J., Linnik, O., Louveaux, M., Roberts, I.M., Chapman, S.N. & Oparka, K.J. (2013) Replication and trafficking of a plant virus are coupled at the entrances of plasmodesmata. *Journal of Cell Biology*, 201, 981–995.

Tolia, N.H. & Joshua-Tor, L. (2007) Slicer and the argonautes. *Nature Chemical Biology*, 3, 36–43.

van der Vlugt, R.A.A., Stijger, C.C.M.M., Verhoeven, J.T.J. & Lesemann, D.E. (2000) First report of pepino mosaic virus on tomato. *Plant Disease*, 84, 103.

Voinnet, O. (2005) Non-cell autonomous RNA silencing. *FEBS Letters*, 579, 5858–5871.

Wang, X. (2014) *Phospholipases in plant signaling*, Vol. 20. Berlin/Heidelberg, Germany: Springer.

Wassenegger, M. & Krczal, G. (2006) Nomenclature and functions of RNA-directed RNA polymerases. *Trends in Plant Science*, 11, 142–151.

Willmann, M.R., Endres, M.W., Cook, R.T. & Gregory, B.D. (2011) The functions of RNA-dependent RNA polymerases in Arabidopsis. *The Arabidopsis Book/American Society of Plant Biologists*, 9, e0146.

Xie, Z., Johansen, L.K., Gustafson, A.M., Kasschau, K.D., Lellis, A.D., Zilberman, D. et al. (2004) Genetic and functional diversification of small RNA pathways in plants. *PLoS Biology*, 2, 642–652.

Young, M.D., Wakefield, M.J., Smyth, G.K. & Oshlack, A. (2010) Gene ontology analysis for RNA-seq: accounting for selection bias. *Genome Biology*, 11, R14.

Zanardo, L.G., de Souza, G.B. & Alves, M.S. (2019) Transcriptomics of plant–virus interactions: a review. *Theoretical and Experimental Plant Physiology*, 31, 103–125.

SUPPORTING INFORMATION

Additional supporting information can be found online in the Supporting Information section at the end of this article.

How to cite this article: Alcaide, C., Donaire, L. & Aranda, M.A. (2022) Transcriptome analyses unveiled differential regulation of AGO and DCL genes by pepino mosaic virus strains. *Molecular Plant Pathology*, 23, 1592–1607. Available from: https://doi.org/10.1111/mpp.13249